

Self-organized stable pacemakers near the onset of birhythmicity

Michael Stich, Mads Ipsen, and Alexander S. Mikhailov

Fritz-Haber-Institut der Max-Planck-Gesellschaft, Faradayweg 4-6, D-14195 Berlin, Germany

(November 1, 2018)

General amplitude equations for reaction-diffusion systems near to the soft onset of birhythmicity described by a supercritical pitchfork-Hopf bifurcation are derived. Using these equations and applying singular perturbation theory, we show that stable autonomous pacemakers represent a generic kind of spatiotemporal patterns in such systems. This is verified by numerical simulations, which also show the existence of breathing and swinging pacemaker solutions. The drift of self-organized pacemakers in media with spatial parameter gradients is analytically and numerically investigated.

82.40.Bj, 82.40.Ck, 82.20.Wt

Oscillatory reaction-diffusion systems, such as the Belousov-Zhabotinsky (BZ) chemical reaction, exhibit a rich variety of nonlinear wave patterns. The first complex pattern discovered in this reaction was the target pattern, where concentric waves were emitted by a pacemaker representing a periodic wave source [1]. Subsequently, similar target structures have been observed in many other chemical, physical, and biological systems [2-5]. A simple theoretical explanation of target patterns in oscillatory chemical systems is that their pacemakers are created by impurities which increase the local oscillation frequency in the medium [6]. Most of the target patterns seen in the BZ reaction are indeed caused by small local inhomogeneities, such as dust particles. A general question is whether self-organized target patterns, representing an intrinsic dynamical property, are also possible in reaction-diffusion systems. Examples of stable autonomous pacemakers with localized or extended wave patterns are indeed known for several reaction-diffusion models [7-16].

The aim of the present Letter is to show that stable autonomous pacemakers with extended wave patterns represent a *generic* pattern-forming object in oscillatory reaction-diffusion systems near the onset of *birhythmicity*. Birhythmicity, the coexistence of two stable limit cycles corresponding to uniform oscillations with different frequencies, is possible in various systems [17-20], including glycolytic oscillations [21] and the photosensitive BZ reaction [22]. Here, we derive two coupled amplitude equations yielding the normal form of such a dynamical system near a supercritical pitchfork-Hopf bifurcation which leads to birhythmicity. Using singular perturbation theory, an analytical solution for autonomous pacemakers is then constructed and its stability is numerically confirmed. In addition, target patterns with

breathing or swinging pacemakers are observed. Finally, we show that autonomous pacemakers can drift under the influence of a parameter gradient and determine the drift velocity.

The derivation of normal forms for various kinds of reaction-diffusion systems has recently been discussed by one of the authors [23,24]. Here, we focus our attention on systems near to a supercritical pitchfork-Hopf bifurcation, where a real uniform eigenmode and a pair of complex conjugate uniform eigenmodes start to grow simultaneously. This implies that either a stable small-amplitude limit cycle becomes unstable and gives rise to two stable limit cycles or a pair of stable and unstable limit cycles of small amplitude emerges near to a stable limit cycle. At least three species are needed to realize this bifurcation.

Using the approach described in [23], we have derived the normal form of this bifurcation for a general reaction-diffusion system [25]. The normal form is given by

$$\partial_t A = A - (1 + i\alpha)|A|^2 A + (1 + i\beta)\nabla^2 A + (1 - i\epsilon)Az, \quad (1a)$$

$$\tau\partial_t z = \sigma - \gamma|A|^2 + z - \nu z^3 + \lambda^2\nabla^2 z, \quad (1b)$$

The system (1) represents a complex Ginzburg-Landau equation (CGLE) for a supercritical Hopf bifurcation (1a) which is coupled to an equation describing an imperfect pitchfork bifurcation (1b). Here A is the complex oscillation amplitude and z is the amplitude of the slow real mode. The coefficients τ and λ , respectively, are the ratios of the characteristic time and length scales of the real and the oscillatory mode. The parameter ϵ specifies the frequency shift of the oscillatory mode due to coupling to the real mode, γ characterizes the strength of the feedback from the oscillatory to the real mode, and ν determines the nonlinear saturation of the real mode. When $\sigma = 0$, Eq. (1b) describes a supercritical pitchfork bifurcation, whereas $\sigma \neq 0$ corresponds to an imperfect pitchfork (or “cusp” [26]) bifurcation. Only positive parameters γ, ν , and σ will be considered in this Letter. We assume that uniform oscillations are modulationally stable in this system, i.e. the Benjamin-Feir-Newell condition $1 + \alpha\beta > 0$ is satisfied, and that the waves have positive dispersion, i.e. $\beta - \alpha > 0$.

It can be seen that Eqs. (1) have solutions corresponding to two uniform stable limit-cycle oscillations with frequencies Ω_1 and Ω_3 and to an unstable limit cycle with frequency Ω_2 . The frequencies are given by $\Omega_{1,2,3} = \alpha + (\alpha + \epsilon)z_{1,2,3}$ where $z_{1,2,3}$ are the real roots

of the equation $\nu z^3 - (1 - \gamma)z + \gamma = \sigma$. When $\alpha + \epsilon < 0$ (which is the case that we chose in the simulations), the smallest root z_1 corresponds to the most rapid oscillations, i.e. $\Omega_3 < \Omega_2 < \Omega_1$.

In addition to these uniform oscillations, the system described by Eqs. (1) may have stable nonuniform solutions representing self-organized pacemakers. To create a pacemaker, a sufficiently strong local perturbation should be applied to the state comprised of uniform oscillations with the lower frequency Ω_3 , so that a small core region is formed where oscillations have a higher frequency. Inside this region, the variable z is close to z_1 , whereas outside, it is near to z_3 . The core starts to send out waves and hence a pacemaker is created. The core expands ($\gamma > \sigma$ is a necessary condition for this, otherwise it will contract) and the frequency and the wavenumber of the emitted waves slowly increase at the same time. In turn, this leads to a decrease of the oscillation amplitude of emitted waves. This amplitude controls the propagation velocity of the front, representing the boundary of the expanding core. When a critical wavenumber is reached, the front velocity becomes zero and a stationary pacemaker is formed.

We have constructed an analytical solution for stationary pacemakers in the one-dimensional system (1). The phase ϕ and amplitude ρ are introduced by $A = \rho \exp[-i(\Omega_3 t + \phi)]$. Then ρ is adiabatically eliminated using $\rho^2 \approx 1 + z - (\nabla\phi)^2 + \beta\nabla^2\phi$. The phase equation approximation [27] is valid for smooth phase perturbations and $\nu \gg 1 - \gamma$. Assuming that the characteristic length scale of the real mode, determining the front width, is much shorter than the characteristic length scale of the oscillatory subsystem (i.e. that $\lambda \ll 1$), we apply singular perturbation theory to this problem. The derivation will be published separately [28] and only selected results are reported in this Letter.

The velocity of the front V (of the expanding core) depends on the wavenumber k and is given by

$$V(k) = 3\frac{\lambda}{\tau}\sqrt{\frac{\nu}{2}}\tilde{z}_2(k), \quad (2)$$

where $\tilde{z}_2(k)$ is the middle root of the cubic equation $\nu z^3 - (1 - \gamma + \gamma a)z + \gamma(1 + az_3 - k^2) = \sigma$, with $a = \beta(\alpha + \epsilon)/(1 + \alpha\beta)$. On the other hand, if the core radius R is known, the wavenumber k of emitted waves can be analytically found if the condition $\lambda k \ll 1$ is satisfied (cf. [8]). The inverted dependence $R(k)$ and the velocity $V(k)$ are displayed in Fig. 1(a).

For stationary pacemakers, the front velocity V vanishes. This determines the wavenumber k_0 of a stationary pacemaker and thus allows us to find its core radius R_0 . Analytical solutions for these key properties have been constructed. We find that

$$k_0 = \sqrt{1 - \sigma/\gamma + az_3}, \quad (3)$$

$$R_0 = \frac{1 + \alpha\beta}{(\beta - \alpha)\sqrt{k_{\max}^2 - k_0^2}} \tan^{-1}\left(\frac{k_0}{\sqrt{k_{\max}^2 - k_0^2}}\right), \quad (4)$$

where $k_{\max}^2 = (\alpha + \epsilon)(z_1 - z_3)/(\beta - \alpha)$. The frequency Ω_0 of a stationary pacemaker is $\Omega_0 = \Omega_3 + (\beta - \alpha)k_0^2$. The wavenumber k_0 and the radius R_0 of a stationary pacemaker are shown as functions of the coupling coefficient γ in Fig. 1(b).

Examining the constructed solutions, we note that generally $\Omega_3 < \Omega_0 < \Omega_1$. The frequency Ω_0 of a stationary pacemaker approaches the frequency Ω_1 of rapid uniform oscillations, when the core radius $R_0 \rightarrow \infty$ (and $k_0 \rightarrow k_{\max}$). On the other hand, when the core is small, k_0 is small and the frequency Ω_0 is close to Ω_3 . Stationary pacemakers exist inside an interval of the coupling intensity γ [see Fig. 1(b)]. Our approximate analysis based on singular perturbation theory is only valid when the core is not too small, i.e. $R_0 \gg \lambda$.

Some conclusions about the stability of stationary pacemakers can already be drawn from Fig. 1(a). Suppose the radius R has increased above the stationary radius R_0 . This leads to an increase of the wavenumber k of emitted waves which, in turn, will make the front velocity V negative. Therefore the front will retreat, decreasing the radius R back to its stationary value. This argument is, however, only applicable when the characteristic time scale of the core evolution is much longer than the time needed for the wave pattern to adjust to its changes, i.e. when $\tau \gg 1$. Generally, the stability of stationary pacemakers should be numerically investigated.

The system described by Eqs. (1) was integrated with an explicit Euler scheme where the Laplacian operator was discretized with a nearest-neighbor approximation. No-flux boundary conditions were used. Figure 2(a) displays the evolution of a stationary pacemaker from a small initial perturbation of the real mode z . In the first stage, the core grows with approximately constant speed. Later, the growth is terminated and a stationary object is formed. Figure 2(b) displays the creation and emission of waves in the oscillatory subsystem. The profile of the asymptotic stable stationary pacemaker is shown in Fig. 2(c).

Pacemakers are stable for sufficiently large τ . When τ is decreased, numerical integrations show that stationary pacemakers become unstable. Close to the instability boundary, stable breathing and swinging pacemakers were found [Figs. 3(a)–3(b)]. For a breathing pacemaker, the center remains stationary whereas the radius oscillates. For swinging pacemakers, the radius stays approximately constant while the position of the pacemaker oscillates. Further lowering of τ leads to the disappearance of any stable pacemaker solutions.

Similar to plane waves in the CGLE [29], the waves emitted by a pacemaker may become unstable when their

wavenumber k_0 exceeds the Eckhaus wavenumber given by $k_{\text{EH}} \approx \sqrt{(1+z_3)(1+\alpha\beta)(3+\alpha\beta+2\alpha^2)^{-1}}$. Among other effects, this may lead to the destabilization of a stationary pacemaker, as illustrated by Figs. 3(c)–3(d). Phase singularities and thus oscillation amplitude defects are periodically generated at the core boundary, giving rise to a short-wavelength regime in the core and to a long-wavelength regime in the periphery. The core gradually grows and eventually the whole medium is occupied by rapid uniform oscillations.

In contrast to pacemakers which are created by local heterogeneities, autonomous pacemakers are not pinned and their location is determined only by the initial conditions. Moreover, such self-organized structures are able to move through the medium when spatial parameter gradients are present. Suppose, for example, that the parameter γ varies with a constant gradient κ , i.e. $\gamma(x) = \gamma_0 + \kappa(x - x_0)$, where γ_0 is the value of γ in the center of the pacemaker. For sufficiently small gradients ($\kappa R_0 \ll \gamma_0$), linear perturbation theory can be used. Its application (see [28]) allows us to determine analytically the drift velocity V_{D} as $V_{\text{D}} = \kappa R_0 \partial_{\gamma} V(\gamma_0, k_0)$ where $V(\gamma, k)$ is the front velocity given by Eq. (2).

The simulation displayed in Fig. 4(a) was initiated with a stable stationary pacemaker. After a constant gradient in the parameter γ was introduced, the pacemaker drifted through the medium in the direction of increasing γ . When the gradient was removed, the drift of the pacemaker terminated and a spatially shifted stationary pacemaker was recovered. The emission and propagation of waves persisted during the drift [Fig. 4(b)]. In addition, the Doppler effect led to a small increase of k in the direction of motion.

In this Letter, we have analytically constructed self-organized pacemaker solutions in the vicinity of a pitchfork-Hopf bifurcation. Our numerical investigations have shown that such self-organized patterns are stable for a wide range of parameters. To create autonomous pacemakers, a sufficiently strong local perturbation should be applied to the state corresponding to stable uniform oscillations. This is in contrast to [15], where autonomous target patterns were found near a Hopf bifurcation with a finite wavenumber and thus uniform oscillations of the medium were absolutely unstable. Our approach is also different from the model [10,11] that was constructed to explain target pattern formation in electrohydrodynamic convection and which is based on a Hopf bifurcation of a cellular spatial structure. On the other hand, Ohta *et al.* [14] have investigated a two-component activator-inhibitor model with coexistence of excitable kinetics and stable uniform oscillations, and reported several different kinds of autonomous wave sources. The subsequent numerical studies [30] have, however, shown that while localized target patterns are stable, target patterns which extend over the whole medium are unstable in the model and slowly evolve into uniform oscillations. Sta-

ble localized target patterns are also found in the quintic CGLE [12].

Since our analysis is based on general amplitude equations, the results presented here are valid for any reaction-diffusion system near a soft onset of birhythmicity with small-amplitude limit cycles. In a separate publication [25], this analysis will be applied to a particular chemical model system. As in the case of a Turing-Hopf bifurcation, the results of our analysis based on the amplitude equations may remain (qualitatively) applicable even at significant separation from the bifurcation point. Finally, we note that the physical mechanism responsible for the stabilization of pacemakers in the considered system involves a long-range negative feedback, similar to the one necessary for the formation of stable localized spots in reaction-diffusion models with fast inhibitor diffusion. Here, however, an infinite-range inhibition is caused not by diffusion, but by non-damped propagation of waves emitted from the core region. The effect of pacemaker drift in systems with spatial parameter gradients provides a convenient experimental method to identify self-organized pacemakers and distinguish them from other target patterns caused by local heterogeneities in the medium.

The authors thank T. Ohta for an interesting discussion and H. Engel for bringing Ref. [22] to our attention. Financial support of the Humboldt Foundation (Germany) is gratefully acknowledged.

-
- [1] A. N. Zaikin and A. M. Zhabotinsky, *Nature* **255**, 535 (1970).
 - [2] S. Jakubith *et al.*, *Phys. Rev. Lett.* **65**, 3013 (1990).
 - [3] M. Assenheimer and V. Steinberg, *Phys. Rev. Lett.* **70**, 3888 (1993).
 - [4] S. Nasuno, M. Sano, and Y. Sawada, *J. Phys. Soc. Jpn.* **58**, 1875 (1989).
 - [5] K. J. Lee, *Phys. Rev. Lett.* **79**, 2907 (1997).
 - [6] J. J. Tyson and P. C. Fife, *J. Chem. Phys.* **73**, 2224 (1980).
 - [7] V. A. Vasiliev, Y. M. Romanovsky, D. S. Chernavskii, and V. G. Yakhno, *Autowave Processes in Kinetic Systems* (Reidel, Dordrecht, 1986).
 - [8] A. S. Mikhailov, *Physica D* **55**, 99 (1992).
 - [9] A. L. Kawczynski, W. S. Comstock, and R. J. Field, *Physica D* **54**, 220 (1992).
 - [10] H. Sakaguchi, *Prog. Theor. Phys.* **87**, 241 (1992).
 - [11] H. Kokubo, M. Sano, B. Jانياud, and Y. Sawada, *J. Phys. Soc. Jpn.* **63**, 895 (1994).
 - [12] R. J. Deissler and H. R. Brand, *Phys. Rev. Lett.* **72**, 478 (1994).
 - [13] A. M. Zhabotinsky, M. Dolnik, and I. R. Epstein, *J. Chem. Phys.* **103**, 10306 (1995).
 - [14] T. Ohta, Y. Hayase, and R. Kobayashi, *Phys. Rev. E* **54**,

6074 (1996).

- [15] A. B. Rovinsky, A. M. Zhabotinsky, and I. R. Epstein, *Phys. Rev E* **56**, 2412 (1997).
 [16] O. Nekhamkina and M. Sheintuch, *Physica A* **249**, 134 (1998).
 [17] O. Decroly and A. Goldbeter, *Proc. Natl. Acad. Sci. USA* **79**, 6917 (1982).
 [18] M. Alamgir and I. R. Epstein, *J. Am. Chem. Soc.* **105**, 2500 (1983).
 [19] P. Lamba and J. L. Hudson, *Chem. Eng. Commun.* **32**, 369 (1985).
 [20] C. Pérez-Iratxeta *et al.*, *Biophys. Chem.* **74**, 197 (1998).
 [21] A. Goldbeter, *Biochemical Oscillations and Cellular Rhythms* (Cambridge University Press, Cambridge, 1996).
 [22] H.-J. Krug, L. Pohlmann, and L. Kuhnert, *J. Phys. Chem.* **94**, 4862 (1990).
 [23] M. Ipsen, F. Hynne, and P. G. Sørensen, *Physica D* **136**, 66 (2000).
 [24] M. Ipsen, L. Kramer, and P. G. Sørensen, *Phys. Rep.* **337**, 193 (2000).
 [25] M. Ipsen, M. Stich, and A. S. Mikhailov (to be published).
 [26] Y. A. Kuznetsov, *Elements of Applied Bifurcation Theory* (Springer-Verlag, New York, 1995).
 [27] Y. Kuramoto, *Chemical Oscillations, Waves, and Turbulence* (Springer-Verlag, Berlin, 1984).
 [28] M. Stich, M. Ipsen, and A. S. Mikhailov (to be published).
 [29] B. Janiaud *et al.*, *Physica D* **55**, 269 (1992).
 [30] T. Ohta, private communication.

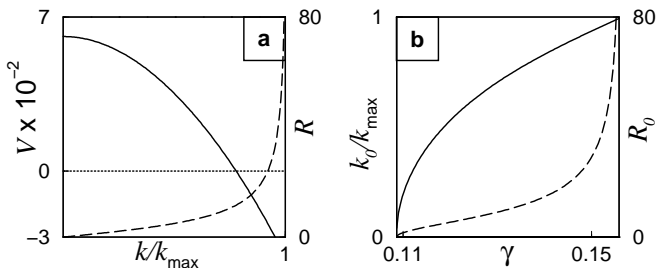


FIG. 1. (a) Dependence of the front velocity V on the wavenumber k of emitted waves (solid line) and dependence of k on the core radius R (dashed line, plotted as R vs. k). (b) The wavenumber k_0 of the waves emitted by a stationary pacemaker (solid line) and the corresponding radius R_0 (dashed line) as functions of the coupling coefficient γ . The parameters are $\alpha = 1.4$, $\beta = 2.3$, $\epsilon = -2.1$, $\lambda = 1$, $\tau = 5$, $\nu = 20$, $\gamma = 0.13$, $\sigma = 0.1$.

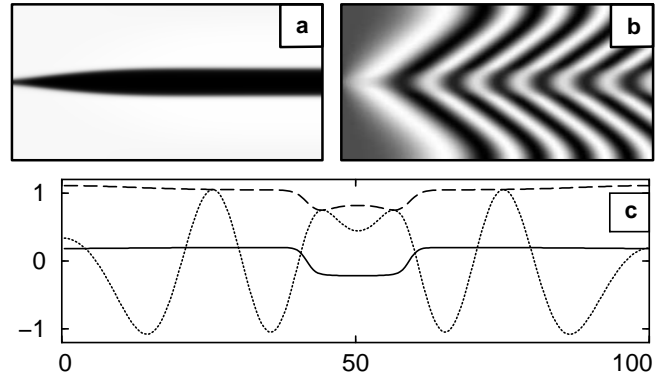


FIG. 2. Development of a stable stationary pacemaker (a,b) and its asymptotic profile (c). Frame (a) shows the evolution of the real mode amplitude z after an initial perturbation. Frame (b) displays the evolution of $\text{Re}A$. In frame (c) the spatial distribution of the variables z (solid line), $\text{Re}A$ (dotted line) and $|A|$ (dashed line) are presented. The system size is $L = 100$ and the time interval is $0 < t < 500$; the same parameters as in Fig. 1. In our gray-scale plots the black and white levels always correspond to the minimum and the maximum values of the plotted variable, respectively. In the space-time plots, time runs along the horizontal axis.

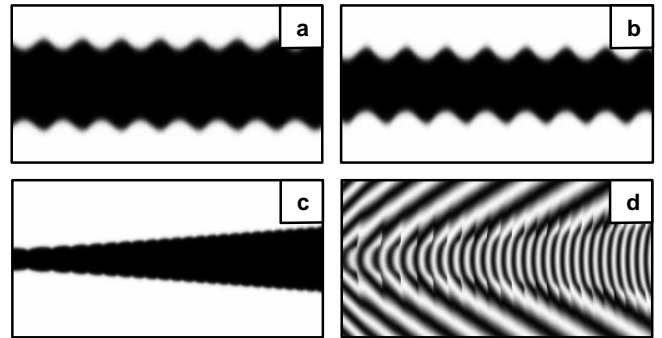


FIG. 3. Breathing (a), swinging (b), and Eckhaus-unstable (c-d) pacemakers. The displayed coordinate and time ranges are $\Delta L = 50$, $\Delta T = 125$ (a-b) and $\Delta L = 100$, $\Delta T = 625$ (c-d). The parameters are $L = 100$, $\alpha = 1.38$, $\epsilon = -3.18$, $\lambda = 0.8$, $\nu = 83$, $\gamma = 5.59 \cdot 10^{-4}$, $\sigma = 3.4 \cdot 10^{-4}$, and for (a): $\beta = 3.0$, $\tau = 0.001$, (b): $\beta = 2.65$, $\tau = 0.001$, (c-d): $\beta = 2.1$, $\tau = 0.025$.

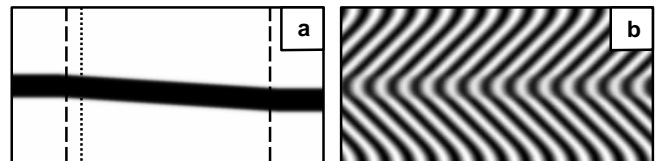


FIG. 4. Drift of a pacemaker. The spatial gradient of the parameter γ with $\kappa/\gamma_0 = 0.003$ is applied inside the time interval indicated by vertical dashed lines in frame (a), which shows the evolution of z in the time interval $0 < t < 2 \cdot 10^5$. The pacemaker is drifting in the direction of increased γ . The parameters are $\gamma_0 = 5.59 \cdot 10^{-4}$, $\beta = 2.3$, $\tau = 2$. The rest are the same as in Fig. 3. Frame (b) displays the drifting wave pattern within a narrow time interval $\Delta T = 500$ during the drift, marked by the dotted vertical line in frame (a).